Remotely Powered Wireless Strain Telemeter

Lokesh A. Gupta* *, David C. Ruddock†, Michael T. Hall†, Farshid Sadeghi† and Dimitrios Peroulis*
*School of Electrical and Computer Engineering, Birck Nanotechnology Center
†School of Mechanical Engineering
Purdue University, West Lafayette, Indiana 47907
Email:{lgupta,druddock,hall42,sadeghi,dperouli}@purdue.edu

***Abstract*—This paper presents a wirelessly powered strain telemeter for mechanical health monitoring applications. The telemter is integrated with a rectenna tuned at 2.4 GHz. The rectenna is comprised by a resonant printed dipole antenna, microstrip transmission line filters and commercially available high-frequency diodes. The experimental results demonstrate that the rectenna is able to deliver 8 mW of DC power to the wireless telemeter when illuminated by a 10-W Yagi transmitter with a gain of 15 dB placed at a distance of over 2.5 m.**

I. Introduction

Continuous health monitoring of moving parts in critical machines is becoming increasingly important because of its potential to become an effective tool for diagnosing faults and predicting failure in real time [1]. Such health monitoring is based on early warning signals and effective algorithms. Health monitoring is critical not only in complex machines commonly found in defense applications, but also in the commercial world. Besides the obvious benefits in safety and security, condition-based rather than time-based maintenance has the potential to significantly decrease wasted time and materials [2].

Strain in mechanical components is one of the most important mechanical parameters that can be monitored and can provide critical information about the health status of a machine. Commercially-available strain sensors have been utilized in a variety of applications including wheel assemblies for estimating the center of gravity in loaded structures. Such strain sensors, however, require either batteries or need to be wired to an external power source [3]. This is undesirable or impossible to do in many applications. Batteries require constant monitoring themselves and external hard-wired power supplies may not be in sealed or hard-to-reach components. To overcome this issue several telemeter-based designs powered through inductive coupling have been proposed [3], [4]. These telemeters typically exhibit a limited operating range in the order of a few inches due to the near-field nature of inductive coupling [3].

The work presented in this paper proposes a new design that aims at remotely powering the sensors at distances over 2 m through a 2.4 GHz rectenna. A similar application for an accelerometer has been shown in [5]. The first rectenna was conceived by Raytheon in 1963 [6]. Since then, numerous advanced rectenna designs with high conversion efficiencies (defined as the ratio of the output DC power divided by the incident power [7]) have been presented. A Rectenna conversion efficiency is a function of the incident RF power, losses across the diode and the antenna gain. The highest conversion efficiency of 90 % at 2.45 GHz was reported by Brown at Raytheon in 1977 [7]. The design used a GaAs-Pt Schottky barrier diode and was tested in a waveguide simulator. McSpadden et al. [7] reported a dipole rectenna at 5.8 GHz with a conversion efficiency of 82 %. Yoo et al. [8] presented a theoretical rectenna design model at 10 GHz and 35 GHz with measured efficiencies of 60 % and 39 % respectively. This work presents for the first time a rectenna integrated with a strain telemeter and powered at a distance of over 2.5 m (Figure 1). Section II presents the design of the proposed system. Section III summarizes the conducted measurements and experimental results.

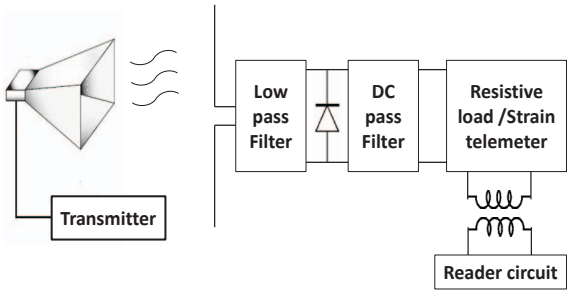

Fig. 1. Wirelessly powered strain telemeter concept. An antenna is used to capture RF power from the transmitter. A diode rectifies the signal and provides DC power to the telemter. The low pass filter is used to block the back scattering of harmonics generated by the non linear diode. A DC pass filter is used after the diode to filter the ripple and provide smooth DC output to the load.

II. Design and Simulation

A. Strain Telemeter

Figure 2 shows a strain telemeter based on the Wein bridge oscillator as reported in [3]. The frequency of this oscillator depends on the resistances and the capacitances in the Wein bridge. The strain sensor shown in Figure 2 is a variable resistor that

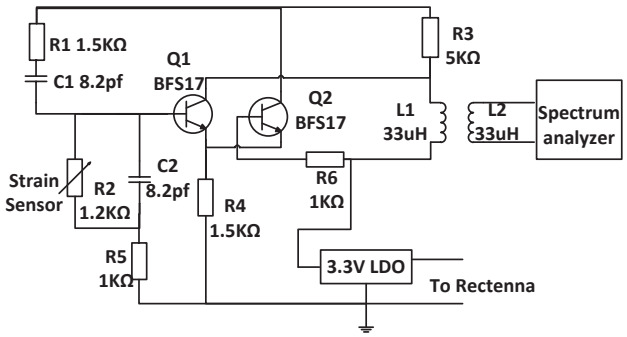

Fig. 2. Circuit diagram for strain telemeter.

depends on the applied strain. This resistor controls the frequency of the oscillator. The resonant frequency is monitored through the inductive coupling link shown in Figure 2. The oscillator circuit is designed using BJT transistors. The power consumption of the strain telemeter is measured to be 8 mW. Thus, the rectenna was designed to capture at least 8 mW of power at 3 m distance from a 10 W Yagi antenna. Furthermore, a 3.3 V low dropout voltage regulator is used to maintain a constant voltage supply to the transistors, thus limiting the noise due to the potential fluctuations of the captured power. The input of the regulator is directly interfaced with the rectenna.

B. Antenna

The antenna is the power capturing element for the rectenna. The antenna needs to have high gain, occupy a minimum area and should be easy to fabricate and integrate with the strain telemeter. The dipole antenna has a reasonable gain for its small size and can be fabricated using standard printed circuit technology. Its omni directionality also enhances the ease of mounting on the telemeter and makes it easy to reach from many angles. Hence, the dipole antenna was selected for the application at hand.

C. Rectifying Diode and DC Pass Filter

The conversion efficiency of a rectenna depends strongly on the specifications of the rectifying diode. The most critical parameters are the diode's forward voltage drop (V_{bi}), zero-biased junction capacitance (C_{j0}), series resistance (R_s), and reverse breakdown voltage (V_{br}). A low forward voltage drop ensures that the diode turns ON and operates in the linear region of the $V_d - I_d$ curve (forward bias region). A high breakdown voltage is critical in applications characterized by high incident power densities. Low junction capacitance and series resistance imply small losses thereby increasing the conversion efficiency of the rectenna. Selection of the diode also involves a tradeoff between V_{br} and C_{j0}. Commercially available diodes that have high V_{br} also have higher C_{j0} that in turn increase the losses. Based on these considerations, the HMPS2820 [9] diode was selected. The ADS [10] built-in non linear diode model was used for design and simulation.

The DC filter is a simple capacitive filter. It filters out the AC components from the pulsating DC, thus providing a smooth DC at the load. The transmission line length between the diode and the capacitor was tuned to cancel out the capacitive reactance of the diode [6]. This also improves the RF to DC conversion efficiency. For this design, a 100 pF capacitor was used.

D. Rectenna Model

In this research, the rectenna was designed using the theoretical model presented in [8] particularly for the initial estimation of the transmission lines [TL] and diode impedances. The initial simulation model was implemented using ideal transmission lines and assuming ideal dipole antenna. The circuit was designed for a 50 Ω load. The ideal dipole antenna was modeled as a simple voltage source with 73 Ω resistor as source impedance. The diode impedance R_d was calculated by (1) [7]

$$R_d = \frac{\pi R_s}{\theta_{on} - sin(\theta_{on})cos(\theta_{on})} \tag{1}$$

where θ_{on} is the dynamic variable dependent on the diode's input power, and R_s is the diode series resistance. The parameter θ_{on} was calculated iteratively by using (2)

$$tan\theta_{on} - \theta_{on} = \frac{\pi R_s}{R_L(1 + \frac{V_{bi}}{V_0})} \tag{2}$$

where R_L is the DC load resistance, and V_0 is the diode self bias DC voltage. V_0 is typically V_{br}/2. Since V_0 was much larger than V_{bi}, V_{bi} was assumed to be approximately zero. The input impedance of the diode was calculated as 49 Ω. The length of transmission lines was required to be small to keep the overall rectenna size minimum. Hence, the electrical length of the transmission line connecting the antenna to the diode was estimated to be 20°. The characteristic impedance of this transmission line was calculated as 70 Ω using impedance matching equations.

The antenna was simulated using Ansoft HFSS [11]. Initially, the length of the dipole antenna was set at λ/2 and a width of 2 mm. The Roger 4003 [12] laminate with a dielectric constant 3.3, thickness of 0.813 mm, and 17 μm thick copper was selected for the substrate. The gap between the dipole terminals was kept equal to the lead spacing between the diode solder pads (0.5 mm). Using HFSS optimization, the length of the dipole was varied to reduce the reactance of the antenna to zero. The simulated antenna gain was 2.1 dB. The impedance of the antenna was 53 Ω at 2.4 GHz. An equivalent lumped-circuit model of the antenna was extracted from HFSS and was used in the ADS circuit simulator. The 73 Ω source resistance of the ideal antenna was replaced by the HFSS lumped-circuit model for more accurate representation of the antenna impedance. The open-circuit voltage of the dipole V_a was calculated by (3) [13]

$$V_a = l_e E_b \tag{3}$$

where E_b is the incident electric field intensity,and l_e is the dipole effective length, which is equal to 0.3183 λ. The electric field intensity was calculated by (4)

$$E_b = \sqrt{\frac{2\eta G_t P_t}{4\pi R^2}} \tag{4}$$

where G_t is the gain of the transmitter (15 dB), P_t is the transmitted power, R is the distance between the transmitter and the receiver, and η is the free space impedance. The simulation model was simulated using transient analysis. Using the ADS tuning option, the electrical length and impedance of the transmission lines connecting the antenna and the diode was optimized for maximum DC voltage across the load. The same process was repeated for the lines connecting the diode to the DC pass capacitor and the DC pass capacitor to the resistive load. Tuning and optimization was performed at 5 V AC input voltage which is approximately half of the reverse breakdown voltage V_{br} [8].

Interfacing of individual components of the rectenna was done using coplanar strip lines (CPS). CPS lines were analyzed by the ADS printed circuit coupled line model. The required impedance and electrical length was achieved by varying the width (w) and the length of the CPS lines. The gap (s) between the metal of the CPS line was set to be equal to the gap between the diode pads. This reduced the parasitic components and made soldering

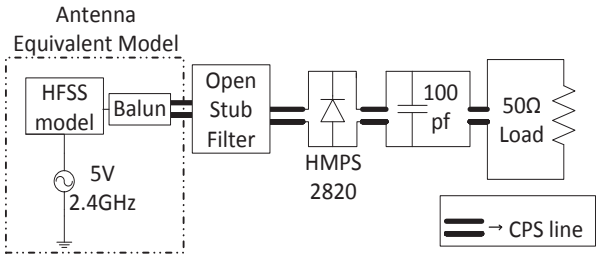

Fig. 3. Simulation model for single rectenna.

easy. An ideal balun was used to interface the unbalanced voltage source to the balanced CPS lines for simulation purposes. The impedance/electrical length was 100 Ω/22^0 for the antenna-diode section, 135 Ω/50^0 for the diode-capacitor section, and 110 Ω/90^0 for the capacitor-load section. The final dimensions are shown in Figure 5.

A diode generates harmonics due to its non-linear characteristics. For the 2^{nd} harmonic (4.8 GHz) the half wave dipole acts like a antenna of size λ that causes back scattering, which results into power loss. To avoid this loss, an open-stub filter was added between the antenna and the diode. The open stub filters are small in size with notch-type response. A similar filter has been pro-

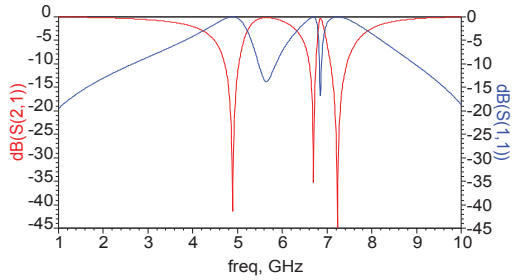

Fig. 4. Stub filter simulation results.

posed and implemented in [14]. The initial length of the tuning stubs was kept at half wavelength of 4.8 GHz and 7.2 GHz with a width of 0.5 mm. Using the ADS tuning and optimization [10] options, the length of the stubs and the gap between the stubs was varied until the required filter response was obtained. Two stubs were implemented for 2^{nd} and 3^{rd} harmonic rejection. Figure 4 shows the S_{11} and S_{21} parameters for the filter.The simulated insertion loss at the 2^{nd} and 3^{rd} harmonics are 25 dB and 28 dB respectively. The passband loss is 0.39 dB at 2.4 GHz.

The filter structure was integrated into the rectenna model (Figure 3). ADS tuning was used to further tune the lengths of stubs to maximize the DC output power. The simulated output power at 5 V source voltage was 22.9 mW without the filter and 25.4 mW with the filter. Implementation of filter increased the simulated output DC power by approximately 10 %.

E. Single and Dual Rectenna

Simulation results showed that the power captured by a single rectenna was less than 8 mW at 3 m distance. Hence, a dual rectenna configuration was designed and implemented. The single rectenna simulation model and layout were replicated on the two sides of the load as shown in Figure 5 to implement the dual

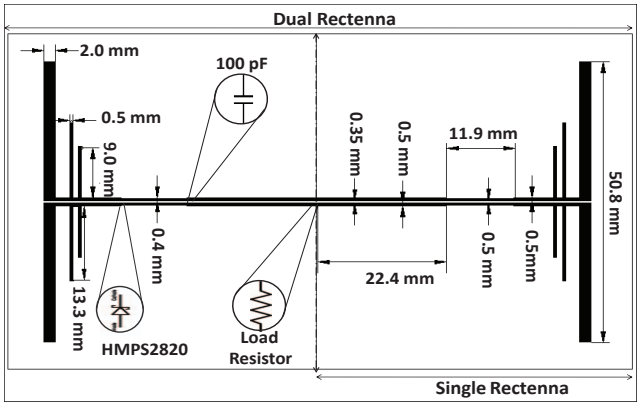

Fig. 5. Rectenna layout.

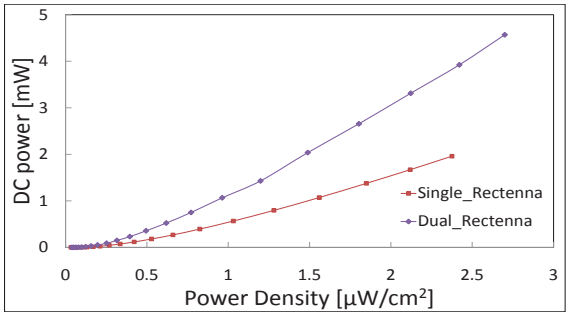

Fig. 6. Simulated DC output power vs. incident power density.

rectenna. Figure 6 shows the simulation results of the output DC power for single and dual rectennas for various incident power densities. The incident power density (P_D) was calculated using Equation (5) [14]

$$P_D = \frac{G_t P_t}{4\pi R^2} \tag{5}$$

III. TEST SETUP AND RESULTS

The testing was done in an open lab environment. Figure 7 shows the block diagram of the test setup. A linearly polarized 15 dB Yagi antenna was used as the transmitter. The antenna was powered by a 43 dB power amplifier through a directional coupler. The attenuated output of the directional coupler was connected to a spectrum analyzer for power measurement. A high-frequency function generator was used as the 2.4 GHz signal source. The rectenna was mounted in a slit on a styrofoam sheet at 3 m distance from transmitter. The sheet was placed at 0.7 m from the ground. The power was varied from −20 dBm to 0 dBm

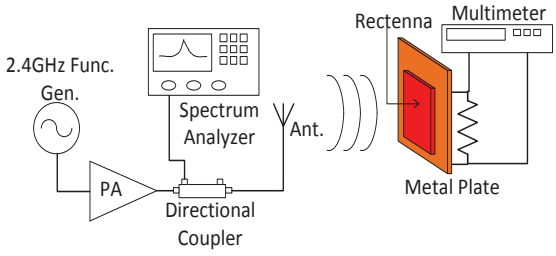

Fig. 7. Test setup block diagram

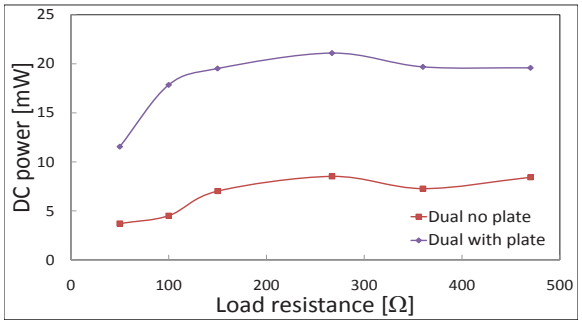

Fig. 8. Measured DC power from dual rectenna as a function of the resistive load.

on the signal generator and the corresponding DC output voltage was measured across the load.

A. *Effect of Reflecting Plate and Resistive Load*

Previous studies on rectennas have shown that the amount of power captured by the rectenna is dependent on the load. The dual rectenna was tested for increasing power densities at 3 m distance from the transmitter for various loads. Figure 8 shows the measured variation of output power vs. resistive load for a 2.67 μW/cm^2 incident power density. These results are in agreement with the rectenna results presented in [7].

The amount of power captured by the rectenna can be increased by placing a metal plate at $\lambda/4$ distance behind the rectenna [15]. Figure 8 shows that the amount of power captured by the rectenna increased 3-4 times with the reflecting plate as compared to the rectenna without the reflecting plate. The drawback of this method is that the antenna is not omnidirectional anymore. The maximum DC power captured by the dual rectenna without and with plate at 3 m distance for the 10 W transmitter was 7.21 mW and 21.1 mW for 267 Ω load respectively.

B. *Strain Telemeter Test and Results*

The resistive load shown in Figure 7 was replaced by the strain telemeter. A 1.2 kΩ semiconductor strain sensor was mounted on a stainless steel beam and was connected to the strain telemeter. The beam was clamped at one end while the free end was loaded with known weights in steps of 1 lbs up to 10 lbs for

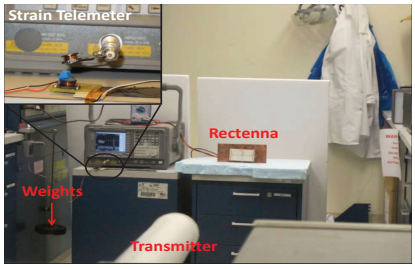

Fig. 9. Test setup with the strain telemeter.

testing the strain in the beam. The reader coil was connected to the spectrum analyzer. For 10 W transmitted power the strain telemeter operated up to 2.54 m. The voltage across the input terminals of the regulator varied from 3.5 V to 4.1 V due to multi path reflections and movement in the lab. Beyond 2.54 m the input voltage across the regular dropped below the minimum specification of the regulator. Figure 9 shows the measurement setup for the complete system. Figure 10 shows the measured results for the strain telemeter for various loads.

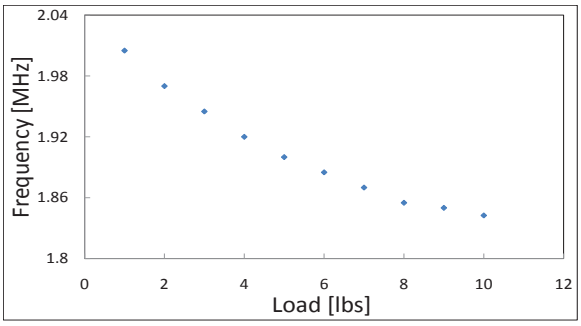

Fig. 10. Measured strain telemeter test results.

IV. Conclusion

In this paper we have demonstrated remote powering of a wireless strain telemeter through a planar rectenna. The design and optimization of the rectenna is presented in detail. The rectenna provides 8 mW to the wireless strain telemeter when powered with 10 W at a distance of more than 2.5 m. The telemeter-rectenna combination successfully identifies load changes even in the presence of multipath effects.

References

[1] L. A. Gupta, "Rectennas and temperature sensors for wireless sensing applications," Master's thesis, Purdue University, West Lafayette, Indiana, Aug 2010.

[2] A. S. Kovacs, "Early-warning wireless telemeter for harsh-environment bearing," Master's Thesis, Purdue University, West Lafayette, Indiana, Dec 2008.

[3] D. C. Ruddock, "Strain telemetry for load identification and center of gravity measurement," Master's thesis, Purdue University, West Lafayette, Indiana, Aug 2010.

[4] A. Joshi, S. Marble, and F. Sadeghi, "Bearing cage temperature measurement using radio telemetry," *Proceedings of the Institution of Mechanical Engineers, Part J: Journal of Engineering Tribology*, vol. 215, no. 5, pp. 471–481, jan 2001.

[5] T. Paing, J. Morroni, A. Dolgov, J. Shin, J. Brannan, R. Zane, and Z. Popovic, "Wirelessly-powered wireless sensor platform," in *Microwave Conference, 2007. European*, 9-12 2007, pp. 999 –1002.

[6] W. C. Brown, "The history of power transmission by radio waves," *Microwave Theory and Techniques, IEEE Transactions on*, vol. 32, no. 9, pp. 1230 – 1242, sep 1984.

[7] J. McSpadden, L. Fan, and K. Chang, "Design and experiments of a high-conversion-efficiency 5.8-ghz rectenna," *Microwave Theory and Techniques, IEEE Transactions on*, vol. 46, no. 12, pp. 2053 –2060, dec 1998.

[8] T.-W. Yoo and K. Chang, "Theoretical and experimental development of 10 and 35 ghz rectennas," *Microwave Theory and Techniques, IEEE Transactions on*, vol. 40, no. 6, pp. 1259 –1266, jun 1992.

[9] "Avago technologies," http://www.avagotech.com, 2010.

[10] "Agilent advanced design system," www.agilent.com/find/ads, 2010.

[11] "Ansoft hfss," http://www.ansoft.com/products/hf/hfss/, 2010.

[12] "Rogers corporation," http://www.rogerscorp.com, 2010.

[13] C. balanis, *Antenna Theory analysis and design*. Hoboken, New Jersey: A John Wiley & Sons, Inc., publication, 2005, section 2, pp. 27–112.

[14] Y. J. Ren, "Microwave and millimeter-wave rectifying circuit arrays and ultra-wideband antennas for wireless power transmission and communications," Phd thesis, Texas A&M University, may 2007.

[15] J. O. McSpadden, A. M. Brown, K. Chang, and N. Kaya, "Receiving rectifying antenna for the International Space Year - Microwave Energy Transmission in Space (ISY-METS) rocket experiment," *IEEE Aerospace Electronic Systems Magazine*, vol. 9, pp. 36–41, Nov. 1994.